IEEE Access
Multidisciplinary | Rapid Review | Open Access Journal

Received May 19, 2022, accepted June 2, 2022, date of publication June 10, 2022, date of current version June 16, 2022.

Digital Object Identifier 10.1109/ACCESS.2022.3182003

Degradation of Flame-Retardant Cross-Linked Polyethylene Caused by Heat, Gamma-Rays, and Steam

YOSHIMICHI OHKI, (Life Fellow, IEEE), AND NAOSHI HIRAI
Research Institute for Materials Science and Technology, Waseda University, Shinjuku-ku, Tokyo 169-0051, Japan
Corresponding author: Yoshimichi Ohki (yohki@waseda.jp)

This work was supported by the Research Entrusted by the Secretariat of the Nuclear Regulation Authority in Japan.

ABSTRACT Various kinds of polymers are used for electrical insulation in nuclear power plants. They are subjected to thermal and radioactive stresses, depending on their locations. They are also subjected to high-temperature steam in the event of an accident. Regarding this, sheets of flame-retardant cross-linked polyethylene (FR-XLPE) were subjected to heat, gamma-rays, and steam exposure, and their infrared absorption spectra, stress-strain relations, indenter moduli, and permittivity spectra were measured. As a result, the following findings are clarified. The oxidation of FR-XLPE occurs more actively by the gamma-ray irradiation of 250 kGy at 100 °C and 0.1 kGy/h than that of 800 kGy at 25 °C and 10 kGy/h. This result indicates that the low dose rate at the high temperature enhances the diffusion of oxygen into the sample. On the other hand, oxidation and cross-linking proceed at the high dose rate. Such oxidation and cross-linking make FR-XLPE hardened by the formation of three-dimensional structures. Although the charge transport is significantly promoted by the steam exposure at 220 °C, this promotion is suppressed if cross-linked structures were formed beforehand by the prior irradiation with gamma rays.

INDEX TERMS Aging, gamma rays, insulating polymer, mitigation, nuclear power plant, steam exposure.

I. INTRODUCTION

Polymers are used for various purposes in many industrial facilities. They are also used in nuclear power plants (NPPs) for electrical insulation in cables and electrical apparatus and airtight sealing in electrical penetrations. Those in NPPs are subjected to radioactive rays and heat, depending on their locations in a NPP. If an accident occurs, such polymers may also suffer high-temperature steam exposure. However, organic polymers like polyethylene and inorganic ones like silicone rubber are relatively easy to deteriorate in such adverse environments. Therefore, we must clarify the behavior of polymers when exposed to the above three stresses.

In many countries, including Japan, once electric cables or electrical penetrations for use in NPPs acquired type approval at the time of laying, they are judged to be usable for each specified operation period without receiving any reliable inspection. Many NPPs in the world began operation in the 1970s. Regarding this, in the mid-2000s, the degradation of polymeric insulation in cables and penetrations became a concern of nuclear regulatory authorities in each country because the end of the initial operation periods of NPPs was approaching [1]. From such a background, recently, large-scale research on polymeric insulating materials for use in NPPs has been conducted at least in Europe, the USA, and Japan. In Europe, the University of Bologna has been playing a leading role in a project called "European Tools and Methodologies for an efficient ageing management of nuclear power plant Cables (Team Cables)" [2], [3], while "Light Water Reactor Sustainability (LWRS) Program" organized by the US DOE has been carried out by many institutes such as Pacific Northwest National Laboratory [4], [5].

Much research has also been carried out in Japan to examine the degradation behavior of various insulating polymers such as silicone rubber (SiR), soft epoxy resin (SE), flame-retardant ethylene-propylene-diene rubber (FR-EPDM), flame-retardant cross-linked polyolefin (FR-XLPO), non-flame-retardant cross-linked polyethylene (NFR-XLPE), and flame-retardant cross-linked polyethylene (FR-XLPE) in a project entrusted by the Nuclear Regulation Authority in Japan [6]–[17]. Here, NFR-XLPE and FR-XLPE are used in both pressurized-water type and boiling-water

The associate editor coordinating the review of this manuscript and approving it for publication was Jinhua Sheng.

type NPPs, in Japan, depending on the purpose of each cable. We have not reported in the form of a refereed paper about the degradation behavior of FR-XLPE placed in a simulated severe accident (SA) environment of NPPs. Regarding this, we describe the above topic in this paper.

II. EXPERIMENTAL METHODS

The samples examined in this research are FR-XLPE, made by a Japanese manufacturing company of boiling-water type NPP-related goods, using the same original materials with the same process. They exhibit the same quality as those used for the electrical insulation of safety-related cables in a boiling-water type NPP in Japan. Unless otherwise mentioned, they are in the shape of a sheet with a thickness between 0.5 and 1.0 mm and a size suitable for each measurement. We combined heat, irradiation with ^{60}Co gamma rays, and exposure to high-temperature steam containing no oxygens as an aging treatment given to each sample sheet. Their combinations, listed in Table 1, were determined by referring to the most severe accident conditions envisioned in a restart review of a NPP in Japan [18]. More in detail, 155 °C is an assumed highest temperature during a severe accident, whereas 220 °C was chosen as a temperature higher than the design limit temperature of the containment vessel of a NPP.

In Table 1, C denotes accelerated irradiation for simulating the normal operation of a NPP for 40 years. In addition, R and S represent the simulated gamma-ray irradiation and steam exposure during a SA, respectively. If necessary, we distinguish the temperature and pressure of the steam by adding 1 and 2 to the letter S. In a possible SA, C and S occur simultaneously. However, it is difficult in experiments to provide them simultaneously to a sample sheet. Therefore, S1 or S2 always follows C when we simulate a SA. Relating to this, the sheet subjected to C and S1 in this order is called CS1. Likewise, sample CRS1 denotes that the sample sheet was subjected to C, R, and S1 in this order.

For pristine unaged sample sheets, several chemical analyses were conducted to obtain information about the compositions of the present FR-XLPE. In addition, for sample sheets before and after the above irradiation or steam exposure or their combination, we measure Fourier transform mid-infrared absorption (FT-MIR) spectra in an attenuated total reflection (ATR) mode at wave numbers from 600 to 4000 cm^{-1} using a spectrometer (FT/IR-4200, JASCO) at room temperature.

As a principal measurement method, we carried out a tensile test at room temperature in air to measure the elongation at break (EAB) and the tensile strength (TS). For this purpose, a dumbbell-shaped sample sheet was cut from an unaged sheet. Then the above irradiation, steam exposure, or their combination was given to the sheet. Here, EAB and TS were measured as specified by a Japanese industrial standard [19] at a tensile speed of 500 mm/min using a universal tester (5565, Instron).

In addition, we measured the indenter modulus (IM) at room temperature in air to examine the surface hardness using an indenter (IM-INSS III, Tobusa Systems) equipped with a needle with a tip diameter of 0.79 mm. Here, IM in N/mm is defined as a pushing force needed to push the needle by 1.0 mm deeper into the sample surface at a speed of 0.080 mm/s when the pushing force is in a range from 1.0 to 4.0 N [20].

Furthermore, the real and imaginary parts of complex relative permittivity, or the relative dielectric constant ε_r' and dielectric loss factor ε_r'', were measured for a sample sheet in the shape of a square of 4 cm × 4 cm. A circular aluminum electrode with a diameter of 20 mm was attached to each surface with silicone oil. The measurement was carried out at various temperatures from 25 to 200 °C at intervals of 25 °C in a vacuum by applying an ac 3 V at frequencies from 10^{-2} to 10^5 Hz using an impedance analyzer (SI126096W, Solartron).

TABLE 1. Samples and aging conditions of FR-XLPE.

	Irradiation			Steam Exposure			
Name	T[a]	DR[b]	TD[c]	T[a]	P[d]	D[e]	Sy[f]
	°C	kGy/h	kGy	°C	MPaG	Day	
U	--	--	--	--	--	--	○
C	100	0.1	250	--	--	--	△
R	25	10	800	--	--	--	□
CR	--	--	1050	--	--	--	△
S1	--	--	--	155	0.44	7	●
S2	--	--	--	220	0.62	7	●
RS1	25	10	800	155	0.44	7	■
RS2	25	10	800	220	0.62	7	■
CRS1	--	--	1050	155	0.44	7	⬟
CRS2	--	--	1050	220	0.62	7	⬟

[a]T: Temperature, [b]DR: Dose Rate, [c]TD: Total Dose, [d]P: Pressure, [e]D: Duration, [f]Sy: Symbol

III. RESULTS

A. INSTRUMENTAL ANALYSES

Although we cannot disclose all the results of our instrumental analyses due to the non-disclosure agreement, we found that the present FR-XLPE contains ethylene-bis(tetrabromophthalimide) (EBTBPI) and Sb_2O_3 as flame retardants. It also contains talc as an inorganic filler. These additives seem not peculiar to the present samples since we often found them in ordinary NFR-XLPE or FR-XLPE. We also found in the present FR-XLPE several points different from NFR-XLPE. First, it is black and completely opaque. This is a clear difference from the ordinary colorless and transparent NFR-XLPE [8], which is also used in NPPs for electrical insulation. Secondly, it is much softer than NFR-XLPE, as will be revealed later in this paper. The reason for these points is that FR-XLPE contains some rubber, although we could not identify its composition. In this regard, we had better consider that FR-XLPE is a kind of compound of XLPE and rubber.

As three typical examples of the FT-MIR spectra exhibiting significant changes compared to the undegraded sample U,

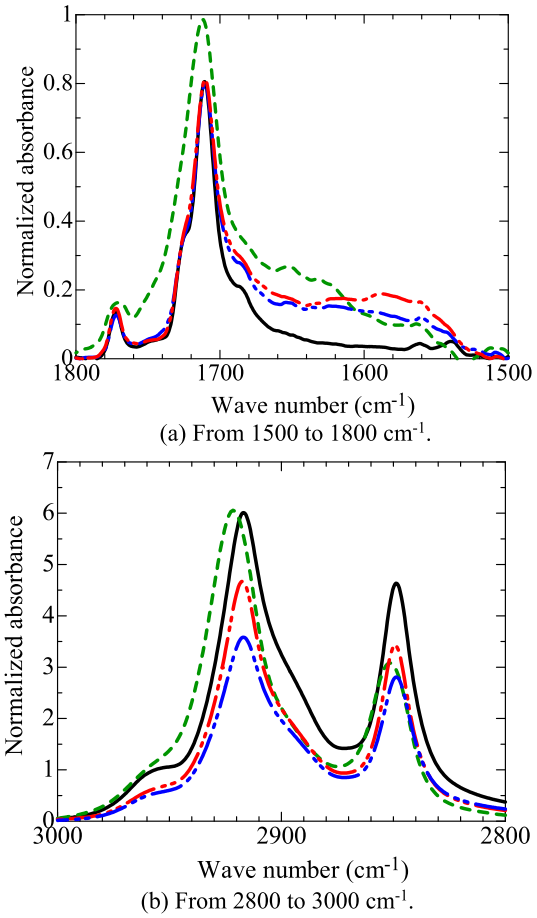

FIGURE 1. FT-MIR absorption spectra normalized by the absorbance at 1020 cm^{-1} in wave number ranges from 1500 to 1800 cm^{-1} (a) and 2800 to 3000 cm^{-1} (b). U (——), CR (– – –), CRS1 (-·-), and CRS2 (-·——).

those obtained for samples CR, CRS1, and CRS2 are shown. Here, Figs. 1(a) and 1(b) are the spectra in wave number ranges from 1500 to 1800 cm^{-1} and 2800 to 3000 cm^{-1}, respectively. Each spectrum is the average of two spectra measured at two points on the surface of the same sample sheet and its intensity was normalized by the intensity at 1020 cm^{-1} due to talc included in the sample as an additive [21]. The absorption at 2848 cm^{-1} and that at 2917 cm^{-1} are due to the symmetric and asymmetric vibrations of CH_2, respectively [22], while the absorption at 1709 cm^{-1} and that at 1735 cm^{-1} are both due to carbonyl groups; in carboxylic acid and carboxylic acid ester, respectively [23]. To confirm the abundance of carbonyl groups generated by the oxidation, the area below the straight line connecting the absorption at 1500 cm^{-1} and that at 1800 cm^{-1} was subtracted as the base absorption from each spectral waveform, and then the remaining waveform was separated by assuming several Lorentz functions. As a result, we obtained the absorption component with a peak at 1709 cm^{-1} and the one with a peak at 1735 cm^{-1}. By assuming that the two components are due to carbonyl groups [23], the sum of their whole areas was calculated as the integrated abundance of carbonyl groups.

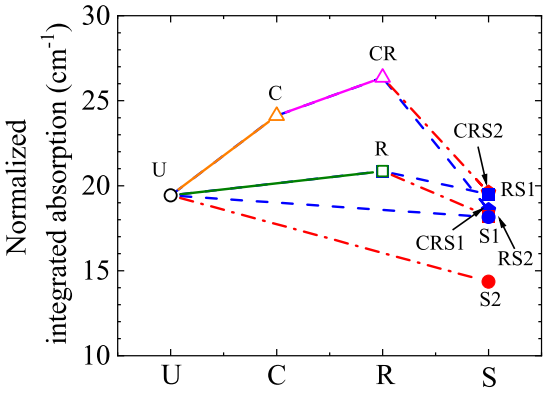

FIGURE 2. Normalized integrated absorption of carbonyl groups measured by FT-MIR. U (○), C (△), R (□), CR (△), S1 (●), S2 (●), RS1 (■), RS2 (■), CRS1 (⬟), and CRS2 (⬟).

Fig. 2 shows the resultantly obtained sample dependence of the normalized intensity of integrated absorption due to carbonyl groups. Compared with the undegraded sample U, the normalized intensity becomes high in sample R irradiated to 800 kGy under the condition of room temperature and high-dose-rate. It becomes much higher in sample C irradiated to 250 kGy under the condition of high temperature and low dose rate and even much higher in sample CR irradiated to 1050 kGy under the conditions of high-temperature/low-dose-rate and subsequently room-temperature/high-dose-rate. The fact that the normalized intensity becomes higher by the irradiation of 250 kGy at 100 °C and 0.1 kGy/h in sample C than that of 800 kGy at 25 °C and 10 kGy/h in sample R indicates that the oxidation induced by the gamma-ray irradiation is enhanced more at a high temperature and a low dose rate.

On the other hand, the intensity of normalized integrated absorption due to carbonyl groups becomes significantly lower in sample S2 exposed only to steam at 220 °C. It also becomes low in samples RS1, CRS1, RS2, and CRS2, exposed to steam after the gamma-ray irradiation compared to the intensity of each prior sample before the steam exposure.

Next, in order to examine the abundance of the methylene groups, the area below the straight line connecting the absorption at 2800 cm^{-1} and that at 3000 cm^{-1} was subtracted as the base absorption from each spectral waveform, and the sum of the whole areas of the absorption components with peaks at 2848 and 2917 cm^{-1} was calculated as the integrated abundance of methylene groups [22]. As shown in Fig. 3, the abundance of methylene groups is scarcely affected by the gamma-ray irradiation C, R, and CR, or by the steam exposure S2 at 220 °C. On the other hand, it decreases in samples S1, RS1, and CRS1 exposed to steam at 155 °C without or with the prior gamma-ray irradiation. It also decreases in samples RS2 and CRS2 exposed to steam at 220 °C with the prior gamma-ray irradiation.

B. MECHANICAL PROPERTIES

When we do a tensile test, a stress-strain (*S-S*) curve, taking the stress on an ordinate and the strain on an abscissa,

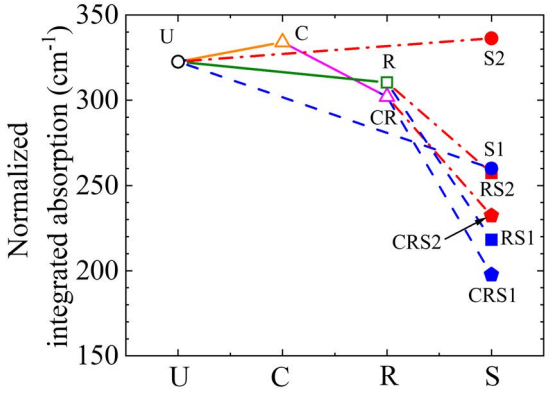

FIGURE 3. Normalized integrated absorption of methylene groups measured by FT-MIR. As for the sample symbols, refer to Table 1 or Figure 2.

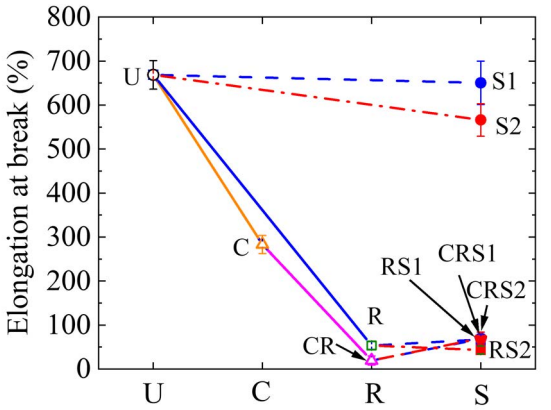

FIGURE 4. Changes in elongation at break of FR-XLPE measured for various samples. As for the sample symbols, refer to Table 1 or Figure 2.

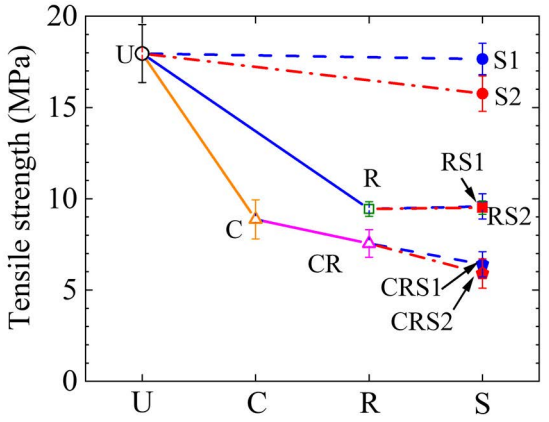

FIGURE 5. Changes in tensile strength of FR-XLPE measured for various samples. As for the sample symbols, refer to Table 1 or Figure 2.

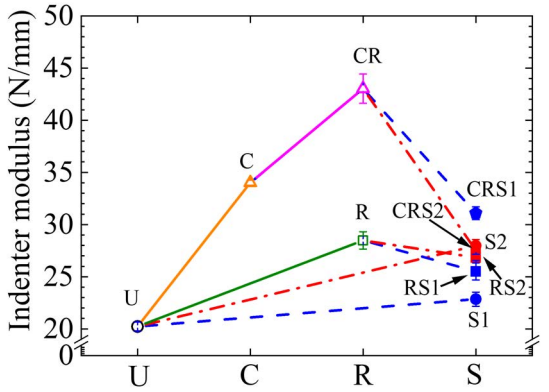

FIGURE 6. Changes in indenter modulus of FR-XLPE measured for various samples. As for the sample symbols, refer to Table 1 or Figure 2.

is drawn. While EAB is defined as the ratio of the length after the elongation to the initial unstretched one, the stress at the time of break is referred to as TS. Fig. 4 shows the average, represented by the symbol, and the standard deviation, represented by the vertical bar, of EAB obtained by measuring five to six *S-S* curves for each sample. In several cases, the bar is smaller than the size of the symbol. While EAB is slightly reduced by the steam exposure at 220 °C (S2), it is significantly reduced by the gamma-ray irradiation. Namely, it decreases to about 0.4 times the initial EAB by irradiation C and less than 0.1 times by irradiation R and CR. Therefore, there is almost no room for the changes in EAB by the subsequent steam exposure.

Fig. 5 shows TS of each sample obtained from the tensile test. Similar to Fig. 4, the symbol and vertical bar represent the average and standard deviation, respectively. Overall, TS exhibits similar trends to EAB. As for the effects of gamma-ray irradiation, TS is almost the same between the condition of high temperature and low dose rate (C) and that of room temperature and high dose rate (R), while EAB is decreased more significantly by R than by C.

Fig. 6 shows the average and the standard deviation of IM measured in various samples. Here, as mentioned in Section II, IM is a parameter that indicates the hardness of the surface of a sample because it is the slope of the force applied to an indenting needle with respect to the indented depth. IM increases in sample C irradiated at the high temperature with the low dose rate, while it increases more significantly in sample CR irradiated first in the same manner as sample C and then further at room temperature with the high dose rate. The irradiation R at room temperature with the high dose rate also increases IM, although not significantly. This is also the case in the steam exposure S1 at 155 °C and S2 at 220 °C. On the other hand, samples CRS1, CRS2, RS1, and RS2 subjected to steam exposure after the gamma-ray irradiation have lower IM values than the corresponding values before the steam exposure.

C. COMPLEX PERMITTIVITY

We measured ε_r' and ε_r'' of all the samples in a wide frequency range from 10^{-2} to 10^5 Hz in a wide temperature range from 25 to 150 °C at intervals of 25 °C. However, to save space, we show only the results measured for samples U, S2, and CR2 in Fig. 7 as three typical examples.

In sample U shown in Fig. 7(a) and sample CRS2 shown in Fig. 7(c), ε_r' increases monotonically as the measurement

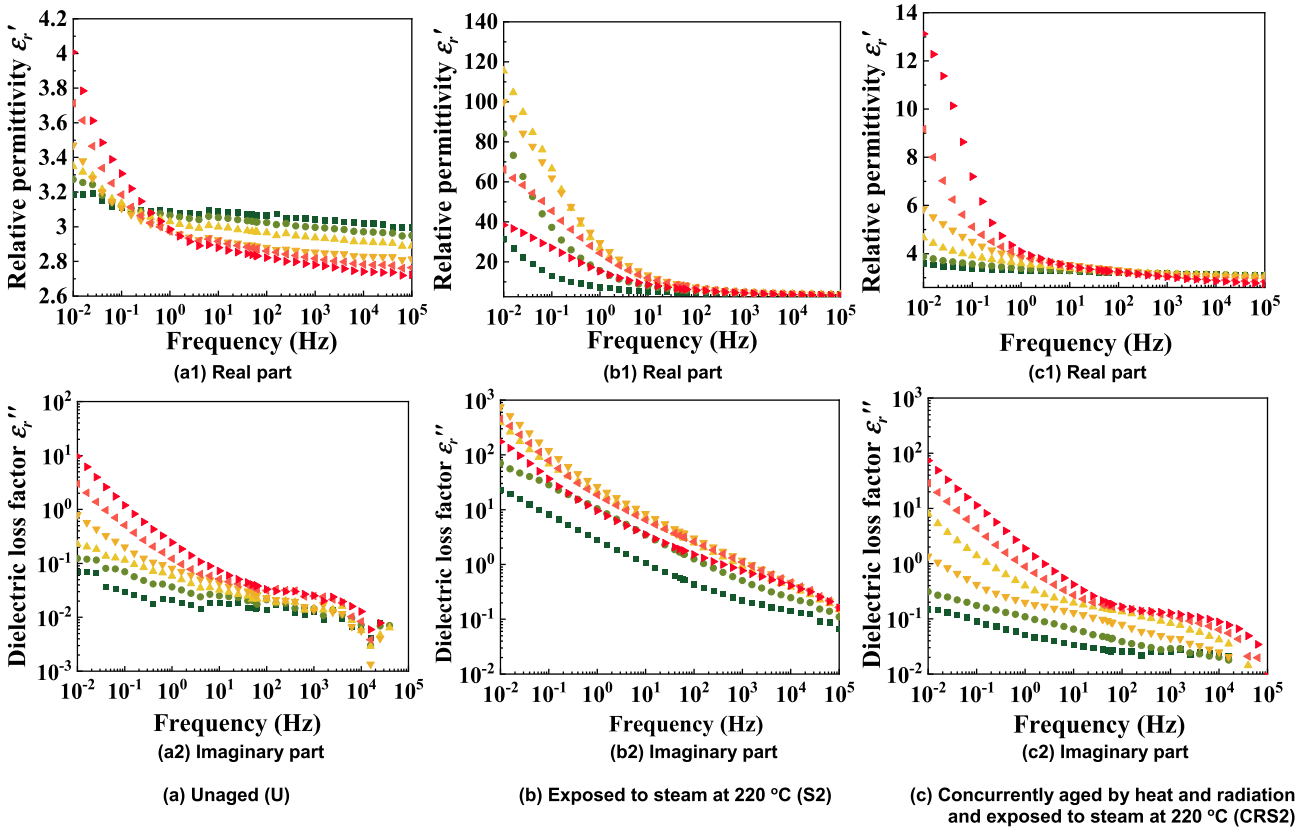

FIGURE 7. Complex permittivity of the unaged sample U (a), S2 exposed to steam at 220 °C (b), and CRS2, concurrently aged by heat and radiation under two conditions and exposed to steam at 220 °C (c), as a function of frequency. 25 (■), 50 (●), 75 (▲), 100 (▼), 125 (◀), and 150 °C (▶).

temperature rises at frequencies lower than sample-dependent frequencies, whereas it decreases monotonically at frequencies higher than the above frequencies. On the other hand, ε_r'' increases in these two samples monotonically in nearly the whole frequency range as the measurement temperature rises. The above changes are slightly different in sample S2 shown in Fig. 7(b). That is, both ε_r' and ε_r'' increase at all frequencies as the measurement temperature rises in a temperature range up to 75 °C, but when the measurement temperature reaches 100 °C or higher, they decrease as measurement temperature increases.

However, regarding the increase in ε_r' and ε_r'' seen in the low-frequency range, ε_r' increases up to 4.0 at 0.01 Hz in the undegraded sample U shown in Fig 7(a) and 13 in CRS2 shown in Fig 7(c). Similarly, ε_r'' increases to 10 and 10^2 at 0.01 Hz in samples U and CRS2, respectively. However, the corresponding increases are more obvious in sample S2 shown in Fig. 7(b). That is, ε_r' and ε_r'' increase to 120 and 10^3 at 0.01 Hz, respectively, at 75 °C, where they become highest.

At such a low frequency of 0.01 Hz, ε_r' and ε_r'' are not narrowly defined by basic dielectric phenomena such as electronic, atomic, and dipolar orientation polarization. Instead, they are affected by the transport of the movable electric charge carriers in the sample [24]–[27]. That is, ε_r' increases accordingly if carriers accumulate and form a heterocharge layer in front of (an) electrode(s). This type of polarization is recently called electrode polarization [25], [27]. On the other hand, Joule heat generates with the transport of charge carriers in a dielectric, which increases ε_r'' of the dielectric. In this case, the resultant increase in ε_r'' is known to be reciprocally proportional to the frequency of the applied voltage [25], [27]. The frequency dependence of ε_r'', shown in Figs. 7(a2), 7(b2), and 7(c2), satisfies this relation, although it is limited to the regions near the lowest frequency and highest ε_r''. Therefore, Figs. 7(b1) and 7(b2) indicate that the carrier transport is highly accelerated in sample S2 exposed to steam at 220 °C. It seems that moisture or some ionic species related to steam exposure would be responsible for the acceleration of carrier transport.

Next, ε_r' and ε_r'' of each sample measured at 150 °C and 0.01 Hz are shown in Fig. 8. The acceleration of carrier transport in sample S2 is clearly reconfirmed. In addition, if we compare ε_r' and ε_r'' between samples S1 and S2 exposed only to steam of two different temperatures, it is clear that the effect of steam exposure on the transport behavior of charge carriers is very different between 155 and 220 °C. Moreover, if we pay attention to ε_r' and ε_r'' of sample S2 exposed to steam of 220 °C and those of the samples RS2 and CRS2 exposed to steam after gamma-ray irradiation,

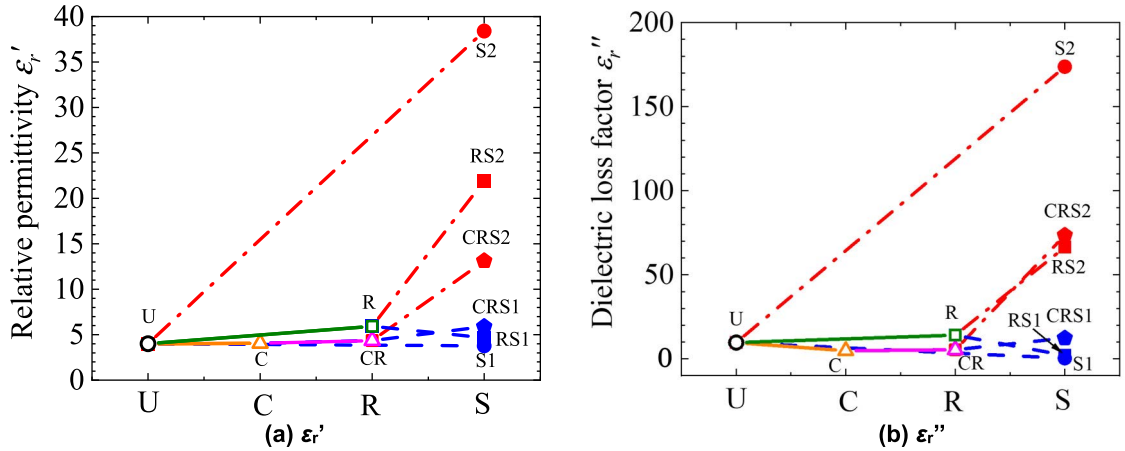

FIGURE 8. Changes in ε_r' (a) and ε_r'' (b) at 150 °C and 0.01 Hz by the aging. As for the sample symbols, refer to Table 1 or Figure 2.

both ε_r' and ε_r'' are lower in samples RS2 and CRS2 than in sample S2. The acceleration of carrier transport seems to be suppressed in samples RS2 and CRS2 compared to sample S2. For an insulating polymer like FR-XLPE, the acceleration of carrier transport is the degradation of its dielectric property. Regarding this, the above suppression of carrier transport is a kind of mitigation of degradation by the gamma rays irradiated before the steam exposure.

IV. DISCUSSION

A. INCLUSION OF RUBBER

As mentioned, we cannot show direct proof of the inclusion of a rubbery additive in the samples. However, the results shown in Figs. 4 and 6 indicate the presence of the rubbery additive in FR-XLPE. Namely, the EAB value of the undegraded sample U, about 670%, is much higher than 300% measured in an undegraded NFR-XLPE sample using the same experimental apparatus [7]. In addition, while IM, an indicator of surface hardness, is about 20 N/mm in sample U, it is about 110 N/mm in undegraded NFR-XLPE [7]. Such high EAB and low IM indicate that FR-XLPE contains a stretchable and soft rubber.

In Fig. 7, ε_r' of sample U at a commercial frequency of 60 Hz at 25 °C is around 3.1, which is much higher than that of 2.1 or 2.5 measured in an undegraded NFR-XLPE [7], [8]. Similarly, ε_r'' of sample U at 60 Hz and 25 °C shown in Fig. 7 is much higher than that measured in the undegraded NFR-XLPE [7], [8]. These facts also indicate that FR-XLPE contains rubber.

In the case of high-temperature steam exposure S2 at 220 °C without prior irradiation, the normalized integrated absorption due to carbonyl groups decreases compared to sample U, as shown in Fig. 2. Here, carbonyl groups are usually not present in pristine NFR-XLPE, as confirmed in our previous research [7], [8]. On the other hand, carbonyl groups are seen abundantly in pristine FR-EPDM [10]. Considering these results, the reason for the appearance of carbonyl groups in sample U seems to be due to the presence of rubber in the sample.

B. EFFECTS OF GAMMA RAYS

The ordinate of Fig. 2 represents the absorption due to carbonyl groups normalized by that due to talc. Since inorganic talc is insensitive to heat, gamma-ray radiation, and steam, its absorption is often used as a reference in FT-MIR measurements. Fig. 2 indicates that the number of carbonyl groups increases by the gamma-ray irradiation C, R, and CR. Here, NFR-XLPE is known to be oxidized when it is irradiated with gamma rays in the presence of oxygen [7], [8], [23]. Fig. 2 also indicates that the oxidation proceeds significantly by the irradiation C at the high temperature of 100 °C and the low dose rate of 0.1 kGy/h when we consider that the total dose is much lower in C than in R. High temperature facilitates the diffusion of oxygens from the surface to the inside of a sample, and the low dose rate ensures sufficient time for oxygens to move. For these reasons, the oxidative reaction seems to proceed more by the irradiation C.

As shown in Figs. 4 to 6, EAB and TS become lower, and IM becomes higher by the gamma-ray irradiation. If we compare the effects of the irradiation R at room temperature with the high dose rate and the irradiation C at the high temperature with the low dose rate, R brings about the larger decline of EAB than C, as shown in Fig. 4, and the lower IM, as shown in Fig. 6, although R and C bring about similar TS values as shown in Fig. 5.

It has been reported that XLPE becomes hardened, and its amorphous parts are cross-linked when it is irradiated with gamma rays. It has also been reported that its dielectric constant and dielectric loss factor slightly increase [7], [8], [28]. Taking this into account, it can be assumed that both cross-linking and oxidation occur in the present samples when irradiated with gamma rays. The irradiation R has a lower irradiation temperature, a higher dose rate, and a higher total dose than the irradiation C. Oxygen is less likely to

diffuse into the sample due to the low temperature and high dose rate in the irradiation R compared to the irradiation C. Therefore, oxidation would not proceed so much by the irradiation R, as proved by the results shown in Fig. 2. This, in turn, indicates that, in the irradiation R, cross-linking occurs more dominantly than oxidation, especially inside the sample. Since cross-linked parts become hardened and are not stretchable, sample R exhibits very low EAB. However, oxidation must be dominant at its surface since air is always present near the surface during irradiation. As a result, the surface cross-linking did not proceed so much in sample R, remaining its IM at a relatively low value, as shown in Fig. 6.

C. SYNERGISM OF RADIATION AND STEAM

The present results indicate that the mechanism of degradation induced by the exposure to steam with no air or oxygen (S) differs significantly depending on the steam temperature and the presence or absence of prior irradiation before the steam exposure. In the case of steam exposure S1 at 155 °C without prior irradiation, the obvious change is only the decrease in methylene groups shown in Fig. 3, and scarce changes are seen in Figs. 2, 4 to 6, and 8 as for the carbonyl groups and mechanical or dielectric properties. The decrease in methylene groups seems to reflect the progress of both oxidation and cross-linking.

In ordinary olefinic polymers like PE or XLPE, oxidation occurs dominantly if the polymer is irradiated with gamma rays when oxygen is present sufficiently while cross-linking becomes dominant when oxygen supply is poor [29]. In other words, oxygen acts as a suppressor of cross-linking in olefinic polymers. However, to promote cross-linking of rubber, we add sulfur in the process called vulcanization. That is, cross-linking of rubber is also formed via a third element such as sulfur in the case of vulcanization. Oxygen can work as a third element of cross-linking in the case of rubber, such as silicone rubber [12], [30]. Since the present FR-XLPE contains rubber, we assume that both cross-linking and oxidation occur simultaneously in the present samples.

Although the steam exposure S1 at 155 °C alone does not worsen the mechanical properties so much, if gamma-ray irradiation was given beforehand, it worsens the properties of RS1 and CRS1, as shown in Figs. 4 and 5. If we watch Fig. 6 together, we have recognized that the gamma-ray irradiation C, R, or CR makes FR-XLPE hardened and that the subsequent steam makes it embrittled. We have already observed a similar result in NFR-XLPE [17]. As we mentioned above, gamma-ray irradiation enhances cross-linking and oxidation, depending on the irradiation condition [29]. In the case of cross-linking, the formation of three-dimensional structures makes the sample hard. On the other hand, the formation of polar carbonyl groups enhances the Coulombic forces between chemical chains, which also makes the sample hard [9], [10]. The hardening induced by thermal or radiation aging is popularly observed in many insulating polymers, as demonstrated by the fact that EAB and IM are widely used to monitor the degradation of such polymers [20], [31].

As indicated by the results shown in Figs. 2 and 3, in the samples RS1, RS2, CRS1, and CRS2 that were experienced steam exposure after gamma-ray irradiation, the carbonyl groups generated by the prior irradiation are reduced, and the methylene groups initially present are also significantly reduced by the successive steam exposure, regardless of the temperature of the steam. This indicates that molecular chain breakage occurs in FR-XLPE due to steam exposure, and the sample becomes embrittled.

D. MITIGATION OF DIELECTRIC DEGRADATION

As mentioned in the previous section, ε_r' and ε_r'' at low frequencies like the data below 1.0 Hz, shown in Figs. 7 and 8, are not ascribed to dielectric polarization in its narrow sense, but they are affected by the transport of charge carriers [24]–[27]. Although the metallic band conduction of electronic carriers in conductors depends negatively on the measurement temperature, the electric conduction in polymers is, regardless of whether it is electronic or ionic, generally dominated by a thermal activation process. Therefore, the positive dependence of ε_r' and ε_r'' on the measurement temperature is reasonable, as in the case of our previous report on NFR-XLPE [7].

Here, Fig. 7 shows that the thermally activated values of ε_r' and ε_r'' are much higher in S2 than in the other two samples. The thermal activation of ε_r' and ε_r'' is suppressed in CRS2 compared to S2 in Fig. 7. Similarly, as shown in Fig. 8, the high-temperature steam exposure of S2 at 220 °C increases the values of ε_r' and ε_r'' measured at 150 °C and 0.01 Hz significantly, meaning that S2 enhances the electric conduction so much under the above condition. However, when the sample was irradiated with gamma rays before the steam exposure at 220 °C, the elevation of ε_r' and ε_r'' is suppressed, as demonstrated by the results of samples RS2 and CRS2 shown in Fig. 8. If we watch Figs. 4 and 5, it is clear that samples RS2 and CRS2 have severely deteriorated mechanically and become embrittled compared to S2. That is, although the sequential irradiation with gamma rays and high-temperature exposure to steam degrade FR-XLPE mechanically, the former prior gamma-ray irradiation mitigates the dielectric deterioration induced by the latter high-temperature steam exposure.

The mitigation of degradation is not limited to FR-XLPE but is also seen in many polymers. Of course, the effect of pre-irradiation with gamma rays on the subsequent degradation induced by steam is largely dependent on each polymer. In the case of silicone rubber, prior gamma-ray irradiation can mitigate the hydrolysis induced by the subsequent steam exposure [12]. Similar mitigation occurs in soft epoxy resin [16]. The formation of three-dimensional cross-linked structures induced by the pre-irradiation of gamma rays decelerates the embrittlement or hydrolysis caused by the subsequent steam exposure in silicone rubber and soft epoxy resin [12], [16]. In the case of FR-XLPE, three-dimensional cross-linked

structures seem to suppress the transport of charge carriers. This is reasonable since electric conduction in polymers is enhanced significantly as the polymer becomes softer in its rubbery state at a temperature higher than its glass transition temperature [25]–[27].

However, the mitigation of degradation in the opposite direction appears in FR-EPDM. Namely, FR-EPDM becomes embrittled by the irradiation with gamma rays, and subsequent exposure to high-temperature steam alleviates the embrittle-ment induced by the irradiation [32]. In other words, the degradation of insulating polymers caused in harsh environments and its mitigation vary significantly from one polymer to another. Concerning this, it is desirable that the findings acquired in the present research will lead to the enactment and revision of future nuclear regulations based on even more scientific knowledge.

Lastly, we have already investigated the effects of pure thermal treatment on the present FR-XLPE [6]. Hence, if we can compare these and the present results with those of the samples purely thermally aged and successively steam exposed without being subjected to the gamma-ray irradiation, we would be able to obtain valuable information about the degradation mechanism of FR-XLPE. In addition, we mainly paid attention to mechanical properties in the present research since its theme is the degradation of low-voltage cables used in NPPs. However, it is generally considered that high-field phenomena such as dielectric breakdown strength and electrical treeing must also be clarified for insulating polymers like XLPE. We hope we can do such research as future subjects.

V. CONCLUSION

For obtaining information on the degradation behavior of FR-XLPE, used for electrical insulation in electric cables in NPPs, its sheets were irradiated with gamma rays in two conditions. One condition, C, was the irradiation to a total dose of 250 kGy at a high temperature of 100 °C with a low dose rate of 0.1 kGy/h, which simulated accelerated aging during the normal operation of a NPP, while the other condition, R, was to 800 kGy at room temperature with a high dose rate of 10 kGy/h, which simulated a severe accident environment. The sheets were also exposed to steam exposure at a temperature of 155 or 200 °C. The effects of such irradiation and steam exposure on the chemical structure, mechanical properties, and dielectric properties were investigated.

As a result, oxidation proceeds, and the sample becomes hardened when irradiated in condition C, while oxidation and cross-linking proceed in condition R. Furthermore, regarding the steam exposure, the degradation mechanism differs depending on the steam temperature. The presence or absence of prior irradiation with gamma rays exerts a big effect on the degradation. Namely, charge transport is significantly promoted by the high-temperature steam exposure, but if cross-linked structures were formed by the prior irradiation with gamma rays, the charge transport due to subsequent high-temperature steam exposure is suppressed. This means that prior irradiation with gamma rays mitigates the dielectric degradation.

ACKNOWLEDGMENT

The authors would like to thank Yu Miyazaki and Mr. Zhenyu Yang for sharing their experimental results.

REFERENCES

[1] Accessed: Apr. 27, 2022. [Online]. Available: https://www.oecd-nea.org/jcms/pl_25708/stress-corrosion-cracking-and-cable-ageing-project-scap
[2] Accessed: Apr. 27, 2022. [Online]. Available: https://www.team-cables.eu/
[3] S. V. Suraci, D. Fabiani, A. Xu, S. Roland, and X. Colin, "Ageing assessment of XLPE LV cables for nuclear applications through physico-chemical and electrical measurements," *IEEE Access*, vol. 8, pp. 27086–27096, 2020, doi: 10.1109/ACCESS.2020.2970833.
[4] Accessed: Mar. 3, 2022. [Online]. Available: https://www.energy.gov/ne/nuclear-reactor-technologies/light-water-reactor-sustainability-lwrs-program
[5] S. Liu, L. S. Fifield, and N. Bowler, "Aging mechanisms of filled cross-linked polyethylene (XLPE) cable insulation material exposed to simultaneous thermal and gamma radiation," *Radiat. Phys. Chem.*, vol. 185, Aug. 2021, Art. no. 109486, doi: 10.1016/j.radphyschem.2021.109486.
[6] Z. Yang, T. Kaneko, N. Hirai, and Y. Ohki, "Aging behavior of flame-retardant cross-linked polyethylene in nuclear power plant environments," *IEEJ Trans. Elect. Electron. Eng.*, vol. 14, no. 8, pp. 1133–1138, 2019, doi: 10.1002/tee.22910.
[7] Y. Miyazaki, N. Hirai, and Y. Ohki, "Effects of heat and gamma-rays on mechanical and dielectric properties of cross-linked polyethylene," *IEEE Trans. Dielectr. Electr. Insul.*, vol. 27, no. 6, pp. 1998–2006, Dec. 2020, doi: 10.1109/TDEI.2020.008840.
[8] Z. Liu, Y. Miyazaki, N. Hirai, and Y. Ohki, "Comparison of the effects of heat and gamma irradiation on the degradation of cross-linked polyethylene," *IEEJ Trans. Electr. Electron. Eng.*, vol. 15, pp. 24–29, 2020, doi: 10.1002/tee.23023.
[9] H. Yamaguchi, H. Ishii, N. Hirai, and Y. Ohki, "Degradation of mechanical and dielectric properties of flame-retardant ethylene propylene rubber by thermal aging," *IEEJ Trans. Elect. Electron. Eng.*, vol. 15, no. 1, pp. 488–495, 2020, doi: 10.1002./tee.23079.
[10] J. You, H. Yamaguchi, H. Ishii, N. Hirai, and Y. Ohki, "Degradation of flame-retardant ethylene-propylene-diene rubber by radiation and steam," *IEEJ Trans. Elect. Electron. Eng.*, vol. 15, no. 11, pp. 1572–1579, 2020, doi: 10.1002/tee.23227.
[11] T. Kaneko, S. Ito, T. Minakawa, N. Hirai, and Y. Ohki, "Degradation mechanisms of silicone rubber under different aging conditions," *Polym. Degradation Stability*, vol. 168, Oct. 2019, Art. no. 108936, doi: 10.1016/j.polymdegradstab.2019.108936.
[12] S. Ito, Y. Miyazaki, N. Hirai, and Y. Ohki, "Effects of gamma irradiation on the degradation of silicone rubber by steam exposure," *J. Nucl. Sci. Technol.*, vol. 58, no. 2, pp. 166–172, Feb. 2021, doi: 10.1080/00223131.2020.1815605.
[13] H. Zhou, W. Hanafusa, K. Udo, N. Hirai, and Y. Ohki, "Aging behavior of flame-retardant cross-linked polyolefin under thermal and radiation stresses," *IEEE Trans. Dielectr. Electr. Insul.*, vol. 28, no. 1, pp. 303–309, Feb. 2021, doi: 10.1109/TDEI.2020.009053.
[14] H. Zhou, N. Hirai, and Y. Ohki, "Various characteristics of severely aged flame-retardant cross-linked polyolefin," *IEEJ Trans. Elect. Electron. Eng.*, vol. 16, no. 12, pp. 1556–1562, 2021, doi: 10.1002/tee.23477.
[15] H. Ishii, N. Hirai, and Y. Ohki, "Comparison of degradation behavior between soft and hard epoxy resins," *J. Nucl. Sci. Technol.*, vol. 58, no. 5, pp. 620–628, May 2021, doi: 10.1080/00223131.2020.1848655.
[16] Y. Ohki, H. Ishii, and N. Hirai, "Degradation of soft epoxy resin for cable penetrations induced by simulated severe accidents," *Energies*, vol. 14, no. 21, p. 6932, Oct. 2021, doi: 10.3390/en14216932.
[17] Y. Miyazaki, N. Hirai, and Y. Ohki, "Changes in chemical structure and mechanical properties of cross-linked polyethylene aged under simulated severe accident conditions of a nuclear power plant," *IEEJ Trans. Fundam. Mater.*, vol. 140, no. 9, pp. 445–450, Sep. 2020, doi: 10.1541/ieejfms.140.445.
[18] Nuclear Regulation Authority in Japan, *Analysis of Insulation Performance of Cables under Severe Accident Environmental Conditions*, document NTEC-2019-1002, 2019.

[19] *Japanese Standards Association. Plastics—Test specimens*; Standard JIS K 7139:2009, 2009.
[20] *IEC/IEEE International Standard for Nuclear Power Plants—Instrumentation and Control Important to Safety—Electrical Equipment Condition Monitoring Methods—Part 2: Indenter Modulus*. Standard IEC/IEEE 62582-2:2011+AMD1, 2016.
[21] V. Čavajda, P. Uhlík, A. Derkowski, M. Čaplovičova, J. Madejová, M. Mikula, and T. Ifka, "Influence of grinding and sonication on the crystal structure of talc," *Clays Clay Minerals*, vol. 63, no. 4, pp. 311–327, Aug. 2015, doi: 10.1346/CCMN.2015.0630405.
[22] J. V. Gulmine and L. Akcelrud, "FTIR characterization of aged XLPE," *Polymer Test.*, vol. 25, no. 7, pp. 932–942, 2006, doi: 10.1016/j.polymertesting.2006.05.014.
[23] M. Sugimoto, A. Shimada, H. Kudoh, K. Tamura, and T. Seguchi, "Product analysis for polyethylene degradation by radiation and thermal ageing," *Radiat. Phys. Chem.*, vol. 82, pp. 69–73, Jan. 2013, doi: /10.1016/j.radphyschem.2012.08.009.
[24] S. Hanada, M. Miyamoto, N. Hirai, L. Yang, and Y. Ohki, "Experimental investigation of the degradation mechanism of silicone rubber exposed to heat and gamma rays," *High Voltage*, vol. 2, no. 2, pp. 92–101, Jun. 2017, doi: 10.1049/hve.2017.0009.
[25] F. Tian and Y. Ohki, "Electric modulus powerful tool for analyzing dielectric behavior," *IEEE Trans. Dielectr. Electr. Insul.*, vol. 21, no. 3, pp. 929–931, Jun. 2014, doi: 10.1109/TDEI.2014.6832233.
[26] M. Mudarra, J. Belana, J. C. Canadas, J. A. Diego, and J. Sellares, "Space charge relaxation in polyetherimides by the electric modulus formalism," *J. Appl. Phys.*, vol. 88, no. 8, pp. 4807–4812, 2000, doi: 10.1063/1.1312839.
[27] Y. Ohki, "Broadband complex permittivity and electric modulus spectra for dielectric materials research," *IEEJ Trans. Electr. Electron. Eng.*, vol. 17, no. 7, pp. 958–972, Jul. 2022, doi: 10.1002/tee.23565.
[28] E. Mustafa, R. S. A. Afia, and Z. A. Tamus, "Application of non-destructive condition monitoring techniques on irradiated low voltage unshielded nuclear power cables," *IEEE Access*, vol. 8, pp. 166024–166033, 2020, doi: 10.1109/ACCESS.2020.3022953.
[29] A. Singh, "Irradiation of polyethylene: Some aspects of crosslinking and oxidative degradation," *Radiat. Phys. Chem.*, vol. 56, no. 4, pp. 375–380, 1999, doi: 10.1016/S0969-806X(99)00328-X.
[30] A. Shimada, M. Sugimoto, H. Kudoh, K. Tamura, and T. Seguchi, "Degradation mechanisms of silicone rubber (SiR) by accelerated ageing for cables of nuclear power plant," *IEEE Trans. Dielectr. Electr. Insul.*, vol. 21, no. 1, pp. 16–23, Feb. 2014, doi: 10.1109/TDEI.2013.004177.
[31] N. Hirai and Y. Ohki, "Correlation between indenter modulus and elongation-at-break observed for four electrical insulating polymers," in *Proc. Int. Symp. Elect. Insulating Mater. (ISEIM)*, Toyohashi, Japan, vol. 2, Sep. 2017, pp. 753–756, doi: 10.23919/ISEIM.2017.8166598.
[32] N. Hirai and Y. Ohki, "Mechanical properties of insulation of a flame-retardant ethylene-propylene-diene rubber cable removed from a nuclear power plant," in *Proc. Inst. Electr. Eng. Jpn. Joint Tech. Meeting Dielectr. Electr. Insul. Electr. Wire Power Cable*, vol. 4, Mar. 2022, pp. 1–8.

YOSHIMICHI OHKI (Life Fellow, IEEE) received the Dr.Eng. degree from Waseda University, Tokyo, Japan, in 1978. He joined as a Teaching Staff of the Department of EE, Waseda University, in 1976, and he is currently a Senior Research Professor and a Professor Emeritus. He is also an Honorary Professor with Xi'an Jiaotong University, China. He was a Visiting Scientist at MIT, from 1982 to 1984, and a Senior Fellow of the Japan Science and Technology Agency, from 2006 to 2008. He is a fellow of the Institute of Electrical Engineers of Japan. He was a recipient of many awards, including the IEEE-DEIS Whitehead Memorial Lecture Award, the Prize for Science and Technology awarded by the Minister of Education of Japan, and the Okuma Memorial Academic Award from Waseda University.

NAOSHI HIRAI received the Dr.Eng. degree from Ehime University, Japan, in 1996. He worked as a short-term Expert at Japan International Cooperation Agency, from 1996 to 1998. He started working at Waseda University, Tokyo, Japan, in 2000, and he is currently a Professor with the Research Institute for Materials Science and Technology. He is engaged in research on the electrical properties of polymeric insulating materials. He is a member of the Institute of Electrical Engineers of Japan.